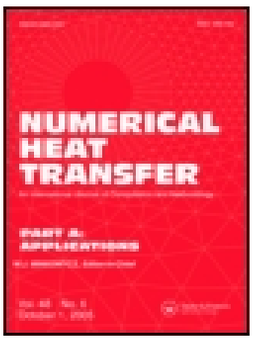

Taylor & Francis
Taylor & Francis Group

Numerical Heat Transfer, Part A: Applications
An International Journal of Computation and Methodology

ISSN: 1040-7782 (Print) 1521-0634 (Online) Journal homepage: http://www.tandfonline.com/loi/unht20

Natural convection of a nanofluid in an enclosure with an inclined local thermal non-equilibrium porous fin considering Buongiorno's model

Hossein Zargartalebi, Mohammad Ghalambaz, Aminreza Noghrehabadi & Ali. J. Chamkha

To cite this article: Hossein Zargartalebi, Mohammad Ghalambaz, Aminreza Noghrehabadi & Ali. J. Chamkha (2016): Natural convection of a nanofluid in an enclosure with an inclined local thermal non-equilibrium porous fin considering Buongiorno's model, Numerical Heat Transfer, Part A: Applications

To link to this article: http://dx.doi.org/10.1080/10407782.2016.1173483

Published online: 13 Jul 2016.

NUMERICAL HEAT TRANSFER, PART A
http://dx.doi.org/10.1080/10407782.2016.1173483

Taylor & Francis
Taylor & Francis Group

Natural convection of a nanofluid in an enclosure with an inclined local thermal non-equilibrium porous fin considering Buongiorno's model

Hossein Zargartalebi[a], Mohammad Ghalambaz[b], Aminreza Noghrehabadi[a], and Ali. J. Chamkha[c,d]

[a]Department of Mechanical Engineering, Shahid Chamran University of Ahvaz, Ahvaz, Iran; [b]Department of Mechanical Engineering, Dezful Branch, Islamic Azad University, Dezful, Iran; [c]Mechanical Engineering Department, Prince Mohammad Bin Fahd University (PMU), Al-Khobar, Kingdom of Saudi Arabia; [d]Prince Sultan Endowment for Energy and Environment, Prince Mohammad Bin Fahd University, Al-Khobar, Kingdom of Saudi Arabia

ABSTRACT

There is growing interest in application of inclined fins to a cavity wall. As such, this paper focuses on the numerical investigation of laminar free convection flow and heat transfer in an enclosure with an inclined thin local thermal non-equilibrium porous fin and saturated by a nanofluid. The porous medium is assumed to be isotropic and homogenous, the cavity walls are assumed to be impermeable to the nanoparticles, and there is a no-slip boundary condition on the enclosure boundaries. The vertical walls are isothermal and the horizontal ones are adiabatic. Moreover, the influence of indispensable parameters regarding heat and mass transfer, such as Rayleigh number, Darcy number, Prandtl number, porosity, thermophoresis and Brownian parameters, fin length, fin position, and the fin angle on the average Nusselt number, are taken into account. Generally, it is found that the average Nusselt number is an increasing function of *Ra, Pr, Da*, and porosity (ε). Furthermore, increasing either fin position (S_p) or thermal conductivity ratio (η) produces corresponding decreases in average Nusselt number. Finally, heat transfer shows a different behavior for different values of fin angles and lengths.

ARTICLE HISTORY
Received 20 December 2015
Accepted 23 February 2016

1. Introduction

Convective flow and buoyancy-induced heat transfer in a square enclosure is a classical problem which has received significant attention in many engineering and fundamental applications comprising solar thermal collector systems, nuclear reactor design, electronic component cooling, paper production, and geothermal systems [1–3]. In a free convection flow, the fluid movement is based on temperature differences and there is no need to any external forces; therefore, the risk of mechanical system failure and also the noise of the fan as external power supply is diminished. In recent investigations, the enhancement of heat transfer through incorporation of attached fins and obstacles to the walls of enclosures has also received much consideration [4–9]. In this regard, Shi and Khodadadi [10] considered the Boussinesq approximation in a steady laminar free convection within a differentially heated square enclosure due to the presence of a solid thin fin, and discovered increased performance of heat transfer when the thin fin, attached to the hot wall, was located in the vicinity of the insulated walls. Oosthuizen and Paul [11] investigated heat transfer in a rectangular enclosure filled with air in which a horizontal plate

CONTACT Mohammad Ghalambaz m.ghalambaz@iaud.ac.ir Assistant Professor at Mechanical Engineering Department, Dezful Branch, Islamic Azad University, Dezful, Iran.
Color versions of one or more of the figures in this article can be found online on at www.tandfonline.com/unht.

Nomenclature

Latin symbols

C	dimensional nanoparticle volume fraction
C_0	dimensional ambient nanoparticle volume fraction
Da	Darcy number
D_B	Brownian diffusion coefficient
D_T	thermophoretic diffusion coefficient
g	gravitational acceleration vector
h_{fs}	interface heat transfer coefficient between the fluid/solid matrix phases
K	permeability of the porous medium
k	thermal conductivity
L	cavity size
L_1	distance between bottom of fin and bottom of cavity
L_2	distance between top of fin and bottom of cavity
Le	Lewis number
L_p	fin length
N_b	Brownian motion parameter
Nhs	Nield number for the fluid/solid matrix interface (fluid/solid matrix interface parameter)
N_r	buoyancy ratio parameter
N_t	thermophoresis parameter
$\overline{Nu}$	average Nusselt number
p	pressure
Pr	Prandtl number
Ra	thermal Rayleigh number
S_p	fin position
$\overline{Sh}$	average Sherwood number
S_s	a special dimensionless coordinate along the walls with its origin at X = 0 and Y = 1 (defined in [10])
T	nanofluid temperature
T_c	temperature at the right wall
T_h	temperature at the left wall
x, y	Cartesian coordinates
u, v	the velocity components along x, y directions

Greek symbols

α	effective thermal diffusivity
β	thermal expansion coefficient
γ_s	modified porous solid matrix thermal conductivity
ε	porosity
θ	non-dimensional temperature
μ	dynamic viscosity
ρ	fluid density
(ρc)	effective heat capacity
η	parameter defined by $\eta = k_s/k_{nf}$
ϕ	relative nanoparticle volume fraction
ψ	fin angle
ζ	non-dimensional parameter defined in Eq. (14)

Subscripts

0	the ambient property
nf	nanofluid phase
p	porous medium
s	solid matrix phase in porous medium

was attached to the cold wall. They discovered that when the plate was either perfectly conductive or adiabatic, heat transfer characteristics were augmented. Nag et al. [7] studied the natural convection heat transfer problem in a differentially heated enclosure with an attached horizontal partition plate. The plate was considered as having been studied under both infinite thermal conductivity and insulated conditions. Whilst placing three partition lengths at three prescribed positions, the applied Rayleigh number range varied between 10^3 and 10^6. They concluded that, regardless of the location of the partition on the hot wall, in the case of a partition of extremely high thermal conductivity the calculated Nusselt number on the cold wall was higher than in the absence of a partition. Moreover, Bilgen [12] using the finite volume method studied natural convection in an enclosure with a thin fin attached on the hot wall. He concluded that Nusselt number was increased as Rayleigh number increased. In addition, Nusselt number was found to be a decreasing function of the relative thermal conductivity ratio and fin length. Furthermore, a laminar, steady, conjugate natural convection in a square cavity with an inclined thin fin of arbitrary length was numerically studied by Ben-Nakhi and Chamkha [13]. The inclined thin fin was located in the middle of the left vertical heated wall. They considered three different fin lengths equal to 20, 35, and 50 percent of the heated surface, representing the influence of the angle and length of the inclined fin and the thermal conductivity of the thick surfaces on the temperature contours and streamlines and Nusselt number, and generally concluded that the presence of the fin decreased average Nusselt number in an unordered way. Ben-Nakhi, with the collaboration of other investigators also implemented in-depth investigations into heat and mass transfer, considering many conditions such as fin length, inclination, and a finned pipe in a cavity [14,15]. Ben Cheikh et al. [16] investigated the effect of inclination on heat transfer and fluid flow in a finned enclosure filled with a dielectric liquid. Chamkha et al. [17] studied the problem of double-diffusive convection in inclined finned triangular porous cavities in the presence of a heat source or sink considering various thermal and concentration boundary conditions. Varol et al. [18] investigated experimentally and numerically natural convection in a square cavity with an attached fin. They observed that heat transfer can be controlled by employing a fin inclined to the wall. In a very recent

work, Khanafer et al. [9] considering a porous fin applied to the hot wall studied laminar natural convection heat transfer in a differentially heated square cavity. Considering the many pertinent parameters such as Darcy number, Rayleigh number, fin inclination length, and angle and the position of the fin, they indicated that to achieve optimal heat transfer, the porous fin should be placed either in the vicinity of the bottom surface or the middle of the vertical hot wall at an angle of 90^0.

In several natural convection applications, when the interaction between the fluid and the porous media is sufficient, the temperature of the solid porous matrix and fluid is much the same. i.e., they are in local thermal equilibrium (LTE). On the other hand, there are many industrial cases in which the temperature difference between the fluid and solid phases was significant, and the local thermal non-equilibrium (LTNE) assumption for the fluid and porous matrix should be taken into account [19–21]. Moreover, in order to enhance the thermal conductivity of the working fluid and consequently heat transfer between the fluid and solid phases, an engineered fluid including nanoparticles, namely nanofluid, has recently been developed. Furthermore, several investigations have been conducted to evaluate the natural heat transfer of nanofluids [22–26]. Buongiorno [27] studied the mass transfer of nanoparticles in nanofluids employing a scale analysis and demonstrated that thermophoresis and Brownian motion are two influential particle transfer mechanisms involved in nanofluids. The thermophoretic force derives from the temperature gradient in the base fluid; the Brownian motion force tends to create uniform nanoparticles in the fluid.

Despite the fact that many researches on natural convection in a cavity have been accomplished, the application of a local thermal non-equilibrium inclined porous fin in a cavity filled with a nanofluid, considering the Buongiorno model, has received almost no attention. As a consequence, the present study aims to analyze the influence of several pertinent parameters such as fin position, inclination angle, Rayleigh number, Brownian and thermophoresis parameters, and thermal conductivity ratio on heat transfer characteristics in a square enclosure.

2. Mathematical formulation

Consider a two-dimensional steady, incompressible natural convection flow in a square cavity saturated by a local thermal non-equilibrium nanofluid in the presence of a porous fin connected to the hot vertical wall. The right vertical wall is assumed to have a constant temperature T_c and the left vertical wall has a constant temperature T_h. Moreover, the horizontal top and bottom walls are insulated, i.e., $\partial T/\partial y = 0$. Due to the no-slip boundary condition, the velocity magnitude on the walls is equal to zero. Further, it is presumed that the enclosure walls are impermeable to the nanoparticles; therefore the mass flux of nanoparticles is zero at the cavity walls. In addition, the nanoparticles are suspended in the nanofluid utilizing a surface charge technology or a surfactant. Indeed, this prevents the nanoparticles from agglomerating on the porous matrix, or agglutination together [28, 29]. The enclosure walls are considered to be rigid, non-conducting, and impermeable. Moreover, the porous matrix is assumed to be isotropic and homogenous throughout the enclosure. Apart from density variation in the buoyancy force which conforms to Boussinesq approximation, the other physical properties of the nanofluid and porous medium are considered to be constant. It is considered that there is a local thermal equilibrium between the base fluid and the nanoparticles, and local thermal non-equilibrium between the porous matrix and the nanofluid. A schematic diagram of the physical domain is represented in Figure 1.

The governing equations comprising the balance laws of momentum and energy, and the conservation of nanoparticles are represented for the fluid and porous domains here in canonical forms as derived by several researchers [27, 30–33]:

Free fluid:

$$\frac{\partial u}{\partial x} + \frac{\partial v}{\partial y} = 0 \tag{1}$$

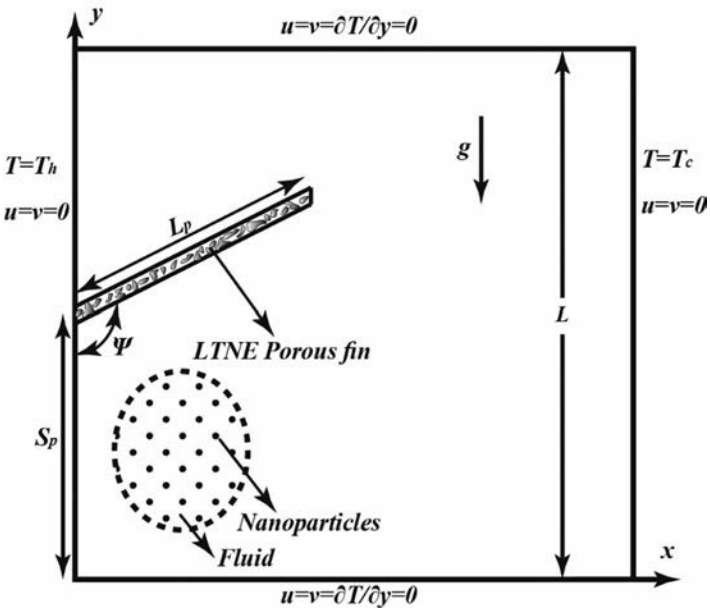

Figure 1. A schematic view of the physical model.

$$\rho_{nf}\left(u\frac{\partial u}{\partial x}+v\frac{\partial u}{\partial y}\right)=-\frac{\partial p}{\partial x}+\mu_{nf}\left(\frac{\partial^2 u}{\partial x^2}+\frac{\partial^2 u}{\partial y^2}\right) \tag{2}$$

$$\rho_{nf}\left(u\frac{\partial v}{\partial x}+v\frac{\partial v}{\partial y}\right)=-\frac{\partial p}{\partial y}+\mu_{nf}\left(\frac{\partial^2 v}{\partial x^2}+\frac{\partial^2 v}{\partial y^2}\right)+\left[-\left(\rho_{p,0}-\rho_{f,0}\right)(C-C_0)+(1-C_0)\rho_{f,0}\beta\left(T_{nf}-T_c\right)\right]g \tag{3}$$

$$u\frac{\partial T_{nf}}{\partial x}+v\frac{\partial T_{nf}}{\partial y}=\frac{1}{(\rho c)_{nf}}\left[\frac{\partial}{\partial x}\left(k_{nf,\infty}\frac{\partial T_{nf}}{\partial x}\right)+\frac{\partial}{\partial y}\left(k_{nf,\infty}\frac{\partial T_{nf}}{\partial y}\right)\right]+\tau\left[D_B\left(\frac{\partial \varphi}{\partial x}\frac{\partial T_{nf}}{\partial x}+\frac{\partial \varphi}{\partial y}\frac{\partial T_{nf}}{\partial y}\right)+\frac{D_T}{T_\infty}\left[\left(\frac{\partial T_{nf}}{\partial x}\right)^2+\left(\frac{\partial T_{nf}}{\partial y}\right)^2\right]\right] \tag{4}$$

$$u\frac{\partial C}{\partial x}+v\frac{\partial C}{\partial y}=D_B\left(\frac{\partial^2 C}{\partial x^2}+\frac{\partial^2 C}{\partial y^2}\right)+\frac{D_T}{T_\infty}\left(\frac{\partial^2 T_{nf}}{\partial x^2}+\frac{\partial^2 T_{nf}}{\partial y^2}\right) \tag{5}$$

Porous fin:

$$\frac{\partial u}{\partial x}+\frac{\partial v}{\partial y}=0 \tag{6}$$

$$\rho_{nf,eff}\left(u\frac{\partial u}{\partial x}+v\frac{\partial u}{\partial y}\right)=-\frac{\partial p}{\partial x}+\mu_{nf,eff}\left(\frac{\partial^2 u}{\partial x^2}+\frac{\partial^2 u}{\partial y^2}\right)-\frac{\mu_{nf,eff}}{K}u \tag{7}$$

$$\rho_{nf,eff}\left(u\frac{\partial v}{\partial x}+v\frac{\partial v}{\partial y}\right)=-\frac{\partial p}{\partial y}+\mu_{nf,eff}\left(\frac{\partial^2 v}{\partial x^2}+\frac{\partial^2 v}{\partial y^2}\right)-\frac{\mu_{nf,eff}}{K}v+\left[-\left(\rho_{p,0}-\rho_{f,0}\right)(C-C_0)+(1-C_0)\rho_{f,0}\beta\left(T_{nf}-T_c\right)\right]g \tag{8}$$

$$\frac{1}{\varepsilon}\left(u\frac{\partial T_{nf}}{\partial x}+v\frac{\partial T_{nf}}{\partial y}\right)=\alpha_f\left(\frac{\partial^2 T_{nf}}{\partial x^2}+\frac{\partial^2 T_{nf}}{\partial y^2}\right)+\tau\left\{D_B\left(\frac{\partial C}{\partial x}\frac{\partial T_{nf}}{\partial x}+\frac{\partial C}{\partial y}\frac{\partial T_{nf}}{\partial y}\right)\right.$$
$$\left.+\left(\frac{D_T}{T_c}\right)\left[\left(\frac{\partial T_{nf}}{\partial x}\right)^2+\left(\frac{\partial T_{nf}}{\partial y}\right)^2\right]\right\}+\frac{h_{fs}(T_s-T_{nf})}{\varepsilon(\rho c)_{nf}} \tag{9}$$

$$0=\alpha_s\left(\frac{\partial^2 T_s}{\partial x^2}+\frac{\partial^2 T_s}{\partial y^2}\right)+\frac{h_{fs}}{(1-\varepsilon)(\rho c)_s}(T_{nf}-T_s) \tag{11}$$

$$\frac{1}{\varepsilon}\left(u\frac{\partial C}{\partial x}+v\frac{\partial C}{\partial y}\right)=D_B\left(\frac{\partial^2 C}{\partial x^2}+\frac{\partial^2 C}{\partial y^2}\right)+\left(\frac{D_T}{T_c}\right)\left(\frac{\partial^2 T_{nf}}{\partial x^2}+\frac{\partial^2 T_{nf}}{\partial y^2}\right) \tag{12}$$

where $\tau=(\rho c)_p/(\rho c)_{nf}$.

3. Nanofluid–porous interface boundary conditions

Several investigations on the appropriate fluid–porous interface boundary conditions for fluid flow and heat transfer phenomena have been accomplished [34]. In the present work, the continuities of velocity and stress are taken into account. Further, it is assumed that heat transfer between the nanofluid and solid matrix at the interface is sufficiently high; consequently, their temperatures are equal as follows [34]:

$$u_{free\,fluid}=u_{porous},\quad v_{free\,fluid}=v_{porous}$$
$$\mu_{nf}\left.\frac{\partial u}{\partial n}\right|_{free\,fluid}=\mu_{nf,eff}\left.\frac{\partial u}{\partial n}\right|_{porous},\quad \mu_{nf}\left.\frac{\partial v}{\partial n}\right|_{free\,fluid}=\mu_{nf,eff}\left.\frac{\partial v}{\partial n}\right|_{porous}$$
$$T_{nf}\big|_{free\,fluid}=T_{nf}\Big|_{porous}=T_s|_{porous} \tag{13}$$
$$k_{nf}\left.\frac{\partial T_{nf}}{\partial n}\right|_{free\,fluid}=k_{nf,eff}\left.\frac{\partial T_{nf}}{\partial n}\right|_{porous}+k_{s,eff}\left.\frac{\partial T_s}{\partial n}\right|_{porous}=q_i$$
$$C_{free\,fluid}=C_{porous},\quad \left.\frac{\partial C}{\partial n}\right|_{free\,fluid}=\left.\frac{\partial C}{\partial n}\right|_{porous}$$

where q_i is total interfacial heat flux, which depicts the heat energy transferred through the porous fin. In addition, the effective thermal conductivity of the nanofluid and the solid matrix can be introduced by $k_{nf,eff}=\varepsilon k_{nf}$, $k_{s,\,eff}=(1\text{-}\varepsilon)k_s$. It is worth mentioning that due to employing a nanofluid in the cavity, interfacial heat transfer between the solid and fluid phases is sufficiently high; therefore, considering the solid and fluid temperatures at the interface to be equal is reasonable [35].

4. Dimensionless equations

In order to non-dimensionalize Eqs. (1)–(13), the dimensional variables are scaled utilizing the ensuing parameters:

$$X=\frac{x}{L},Y=\frac{y}{L},U=\frac{uL}{\alpha_{nf}},V=\frac{vL}{\alpha_{nf}},P=\frac{pL^2}{\rho_{nf}{\alpha_{nf}}^2},\mathrm{Pr}=\frac{\nu_{nf}}{\alpha_{nf}},Da=\frac{K}{L^2},\eta=\frac{k_s}{k_{nf}},$$
$$\zeta_1=\frac{\mu_{nf}}{\mu_{nf,eff}},\zeta_2=\frac{\rho_{nf}}{\rho_{nf,eff}},\phi=\frac{C}{C_0},Ra=\frac{(1-C_0)\rho_{f,0}g\beta\Delta TL^3}{\alpha_{nf}\mu_{nf}}$$

$$\theta_{nf} = \left(T_{nf} - T_c\right)/(T_h - T_c),\ \theta_s = (T_s - T_c)/(T_h - T_c), N_r = \frac{\left(\rho_{p,0} - \rho_{f,0}\right)C_0}{\rho_{f,0}\beta\Delta T(1 - C_0)},\quad N_b = \frac{\tau D_B C_0}{\alpha_f},$$
$$N_t = \frac{\tau D_T \Delta T}{\alpha_{nf}\, T_c}, Nhs = \frac{h_{fs}L^2}{k_{nf}},\ \ \gamma_s = \frac{k_{nf}}{k_s(1 - \varepsilon)}, Le = \frac{\alpha_{nf}}{D_B} \tag{14}$$

Consequently, by substituting Eq. (14) into Eqs. (1)–(13), the governing equations and boundary conditions are turned to dimensionless form as:

Free fluid:

$$\frac{\partial U}{\partial X} + \frac{\partial V}{\partial Y} = 0 \tag{15}$$

$$U\frac{\partial U}{\partial X} + V\frac{\partial U}{\partial Y} = -\frac{\partial P}{\partial X} + \Pr\left(\frac{\partial^2 U}{\partial X^2} + \frac{\partial^2 U}{\partial Y^2}\right) \tag{16}$$

$$U\frac{\partial V}{\partial X} + V\frac{\partial V}{\partial Y} = -\frac{\partial P}{\partial Y} + \Pr\left(\frac{\partial^2 V}{\partial X^2} + \frac{\partial^2 V}{\partial Y^2}\right) - Ra.\Pr.Nr(\phi - 1) + Ra.\Pr.\theta_{nf} \tag{17}$$

$$\begin{aligned} U\frac{\partial \theta_{nf}}{\partial X} + V\frac{\partial \theta_{nf}}{\partial Y} = {} & \left(\frac{\partial^2 \theta_{nf}}{\partial X^2} + \frac{\partial^2 \theta_{nf}}{\partial Y^2}\right) \\ & + Nb\left(\frac{\partial \phi}{\partial X}\frac{\partial \theta_{nf}}{\partial X} + \frac{\partial \phi}{\partial Y}\frac{\partial \theta_{nf}}{\partial Y}\right) + Nt\left[\left(\frac{\partial \theta_{nf}}{\partial X}\right)^2 + \left(\frac{\partial \theta_{nf}}{\partial Y}\right)^2\right] \end{aligned} \tag{18}$$

$$U\frac{\partial \phi}{\partial X} + V\frac{\partial \phi}{\partial Y} = \frac{1}{Le}\left(\frac{\partial^2 \phi}{\partial X^2} + \frac{\partial^2 \phi}{\partial Y^2}\right) + \frac{Nt}{Le \cdot Nb}\left(\frac{\partial^2 \theta_{nf}}{\partial X^2} + \frac{\partial^2 \theta_{nf}}{\partial Y^2}\right) \tag{19}$$

Porous fin:

$$\frac{\partial U}{\partial X} + \frac{\partial V}{\partial Y} = 0 \tag{20}$$

$$U\frac{\partial U}{\partial X} + V\frac{\partial U}{\partial Y} = -\frac{\partial P}{\partial X} + \frac{\zeta_2}{\xi_1}\Pr\left(\frac{\partial^2 U}{\partial X^2} + \frac{\partial^2 U}{\partial Y^2}\right) - \frac{\zeta_2}{\zeta_1}\frac{\Pr}{Da}U \tag{21}$$

$$\begin{aligned} U\frac{\partial V}{\partial X} + V\frac{\partial V}{\partial Y} = {} & -\frac{\partial P}{\partial Y} + \frac{\zeta_2}{\xi_1}\Pr\left(\frac{\partial^2 V}{\partial X^2} + \frac{\partial^2 V}{\partial Y^2}\right) \\ & - \frac{\zeta_2}{\xi_1}\frac{\Pr}{Da}V - \zeta_2 Ra.\Pr.Nr(\phi - 1) + \zeta_2 Ra.\Pr.\theta_{nf} \end{aligned} \tag{22}$$

$$\begin{aligned} & U\frac{\partial \theta_{nf}}{\partial X} + V\frac{\partial \theta_{nf}}{\partial Y} = \varepsilon\left(\frac{\partial^2 \theta_{nf}}{\partial X^2} + \frac{\partial^2 \theta_{nf}}{\partial Y^2}\right) + Nb \times \varepsilon\left(\frac{\partial \phi}{\partial X}\frac{\partial \theta_{nf}}{\partial X} + \frac{\partial \phi}{\partial Y}\frac{\partial \theta_{nf}}{\partial Y}\right) + \\ & Nt \times \varepsilon\left[\left(\frac{\partial \theta_{nf}}{\partial X}\right)^2 + \left(\frac{\partial \theta_{nf}}{\partial Y}\right)^2\right] + Nhs\left(\theta_s - \theta_{nf}\right) \end{aligned} \tag{23}$$

$$0 = \frac{\partial^2 \theta_s}{\partial X^2} + \frac{\partial^2 \theta_s}{\partial Y^2} + Nhs \cdot \gamma_s\left(\theta_{nf} - \theta_s\right) \tag{24}$$

$$U\frac{\partial \phi}{\partial X} + V\frac{\partial \phi}{\partial Y} = \frac{\varepsilon}{Le}\left(\frac{\partial^2 \phi}{\partial X^2} + \frac{\partial^2 \phi}{\partial Y^2}\right) + \frac{Nt \times \varepsilon}{Le \cdot Nb}\left(\frac{\partial^2 \theta_{nf}}{\partial X^2} + \frac{\partial^2 \theta_{nf}}{\partial Y^2}\right) \tag{25}$$

and the dimensionless interfacial boundary conditions become:

$$
\begin{aligned}
&U_{free\,fluid} = U_{porous}\ ,\ V_{free\,fluid} = V_{porous}\\
&\mu_{nf}\left.\frac{\partial U}{\partial N}\right|_{free\,fluid} = \mu_{nf,\,eff}\left.\frac{\partial U}{\partial N}\right|_{porous}\ ,\ \mu_{nf}\left.\frac{\partial V}{\partial N}\right|_{free\,fluid} = \mu_{nf,\,eff}\left.\frac{\partial V}{\partial N}\right|_{porous}\\
&\theta_{nf}\big|_{free\,fluid} = \left.\theta_{nf}\right|_{porous} = \theta_s|_{porous}\\
&\left.\frac{\partial\theta_{nf}}{\partial N}\right|_{free\,fluid} = \varepsilon\left.\frac{\partial\theta_{nf}}{\partial N}\right|_{porous} + (1-\varepsilon)\eta\left.\frac{\partial\theta_s}{\partial N}\right|_{porous} = \frac{q_i L}{k_{nf}\Delta T} = Q_i\\
&\phi_{free\,fluid} = \phi_{porous}\ ,\ \left.\frac{\partial\phi}{\partial N}\right|_{free\,fluid} = \left.\frac{\partial\phi}{\partial N}\right|_{porous}
\end{aligned}
\tag{26}
$$

Further, the dimensionless boundary condition on the vertical and horizontal walls becomes:

$$
\begin{aligned}
&U(0,Y) = V(0,Y) = 0,\ \theta_{nf}(0,Y)=\theta_s(0,Y) = 1,\ N_b\frac{\partial\phi(0,Y)}{\partial X} + N_t\frac{\partial\theta_{nf}(0,Y)}{\partial X} = 0\\
&U(1,Y) = V(1,Y) = 0,\ \theta_{nf}(1,Y)=\theta_s(1,Y) = 0,\ N_b\frac{\partial\phi(1,Y)}{\partial X} + N_t\frac{\partial\theta_{nf}(1,Y)}{\partial X} = 0\\
&U(X,0) = V(X,0) = 0,\ \frac{\partial\theta_{nf}(X,0)}{\partial Y} = \frac{\partial\theta_s(X,0)}{\partial Y} = 0,\ \frac{\partial\phi(X,0)}{\partial Y} = 0\\
&U(X,1) = V(X,1) = 0,\ \frac{\partial\theta_{nf}(X,1)}{\partial Y} = \frac{\partial\theta_s(X,1)}{\partial Y} = 0,\ \frac{\partial\phi(X,1)}{\partial Y} = 0
\end{aligned}
\tag{27}
$$

Of paramount physical importance in this type of problem is the value of average Nusselt number ($\overline{Nu}$) and average Sherwood number ($\overline{Sh}$), which can be defined as follows:

$$
\overline{Nu} = -\int_0^{L_1}\left.\frac{\partial\theta_{nf}}{\partial X}\right|_{X=0}dY - \int_{L_1}^{L_2}\varepsilon\left.\frac{\partial\theta_{nf}}{\partial X}\right|_{X=0}dY - \int_{L_2}^{1}\left.\frac{\partial\theta_{nf}}{\partial X}\right|_{X=0}dY \tag{28}
$$

$$
\overline{Sh} = -\int_0^{L_1}\left.\frac{\partial\phi}{\partial X}\right|_{X=0}dY - \int_{L_1}^{L_2}\varepsilon\left.\frac{\partial\phi}{\partial X}\right|_{X=0}dY - \int_{L_2}^{1}\left.\frac{\partial\phi}{\partial X}\right|_{X=0}dY \tag{29}
$$

It should be noted here that for analysis of Sherwood number it is feasible to study only Nusselt number since at the left and right vertical walls we have $\frac{\partial\phi}{\partial X} = -\frac{N_t}{N_b}\frac{\partial\theta_{nf}}{\partial X}$ considering boundary conditions for ϕ [Eq. (27)]. Hence, the additional examination regarding integral parameters will include only average Nusselt number according to $\overline{Sh} = -\frac{N_t}{N_b}\overline{Nu}$.

5. Method of solution and validation

In order to solve Eqs. (15)–(25) subject to the boundary conditions Eqs. (26)–(27), the finite element method, which is widely employed in solving industrial and environmental fluid mechanics problems, is utilized [36]. Therefore, the aforementioned governing partial differential equations were transformed to a weak form and solved numerically applying the Galerkin finite element method [36]. Further, the Newton–Raphson method was used to solve the discretized equations for the fluid and porous regions. The detailed solution can be found in previous studies [36–38]. Moreover, the computational domain comprises grid points in which the discretized equations are implemented. The non-uniform grid has been used in both the x- and y- directions in which the grid points are clustered near the walls and the porous fin. The iteration process terminates when the residuals

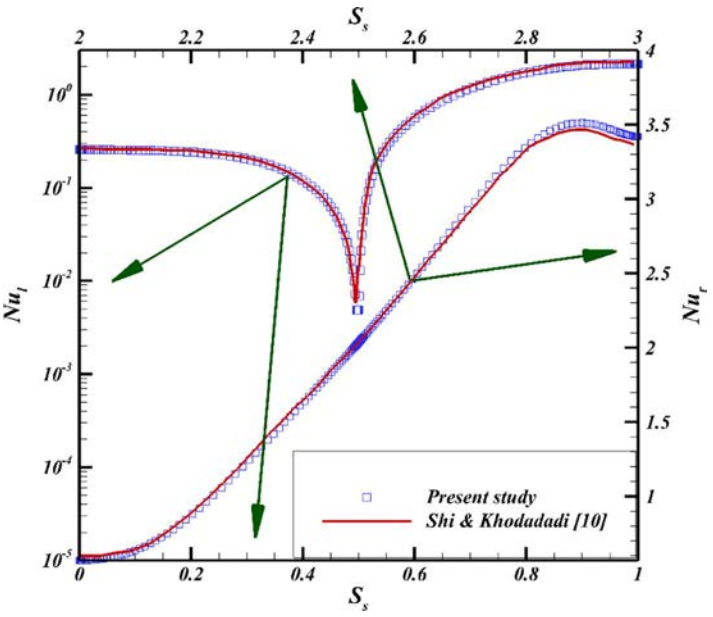

Figure 2. Comprising the variation of local Nusselt number with left (Nu_l) and right (Nu_r) walls of the cavity, $Ra = 10^4$, $L_p = 0.5$, $S_p = 0.5$.

for the dependent variables between two iterations are satisfied by establishing this criterion:

$$\frac{\sum \left|\kappa_{i,j}^{n+1} - \kappa_{i,j}^{n}\right|}{\sum \left|\kappa_{i,j}^{n+1}\right|} \leq 10^{-8} \tag{28}$$

where $\kappa_{i,j}^{n}$ denotes the dependent variables at iteration n. It is worth mentioning that to ensure grid independent results, the problem for different grid sizes was solved and finally the non-uniform mesh of 150×150 was adopted to solve Eqs. (15)–(25).

The present model, in the form of an in-house computational fluid dynamics (CFD) code, has been validated successfully against the work conducted by Shi and Khodadadi [10] in which a steady laminar natural convection in a cavity with an inclined solid fin was studied. In that study [10], the enclosure wall was assumed to be differentially heated, the fin was made of highly conductive materials, and the temperature of the fin was maintained at the same temperature as the attached wall. The computed value of local Nusselt number on the left and right walls is shown in Figure 2. According to Figure 2, the average Nusselt values of the left and right walls computed in the present study are in excellent agreement with the results reported in the literature.

6. Results and discussion

In essence, the presence of a porous fin attached to the enclosure wall affects both flow and heat transfer regimes, and consequently the streamlines, isotherms, and distribution of nanoparticle concentration would be altered relative to a simple cavity with no attached fin (see Figure 3).

According to Figure 3, it is obvious that the inclined porous fin influences the isotherms, concentrations, and streamlines in the enclosure, particularly near the fin. Therefore, variation of fin position (S), angle (Ψ), and length (L_p) affects the flow and heat transfer regimes and consequently, the Nusselt number. The variation of isotherms, concentration contours, and streamlines for the different aforementioned parameters, regarding a porous fin, is not presented for the sake of brevity and instead the

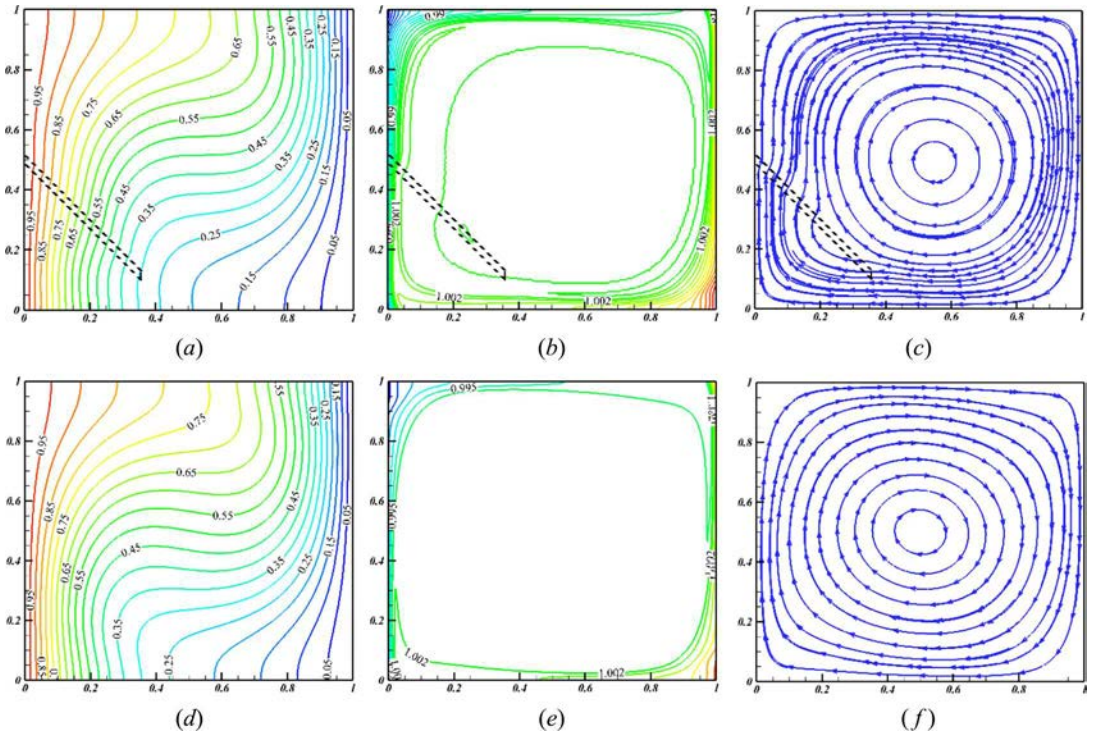

Figure 3. A comparison between isotherms (left), concentrations (middle), and streamlines (right) of two cavities; with attached fin (a–c) and without attached fin (d–f); $Ra = 10^4$, $Pr = 0.1$, $Le = 10^3$, $Da = 10^{-4}$, $\varepsilon = 0.9$, $N_b = 2.5 \times 10^{-4}$, $N_t = 10^{-4}$, $N_r = 5$, Nhs = 5, $\Psi = 45°$, $L_p = S_p = 0.5$.

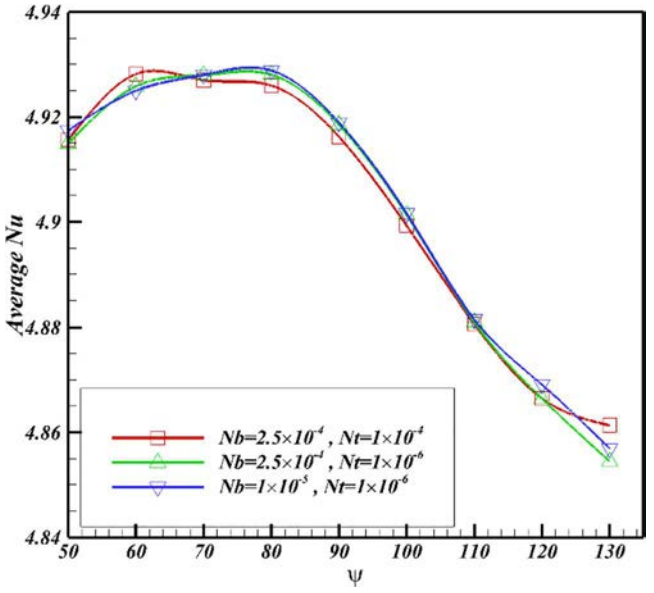

Figure 4. The effect of varying porous fin angle on average Nusselt number for different values of N_b and N_t; $Ra = 10^4$, Pr = 10, $Le = 10^3$, $N_r = 5$, $Da = 10^{-2}$, $\eta = 5$, $\varepsilon = 0.3$, Nhs = 5, $\zeta_1 = \zeta_2 = 0.5$, $L_p = S_p = 0.5$.

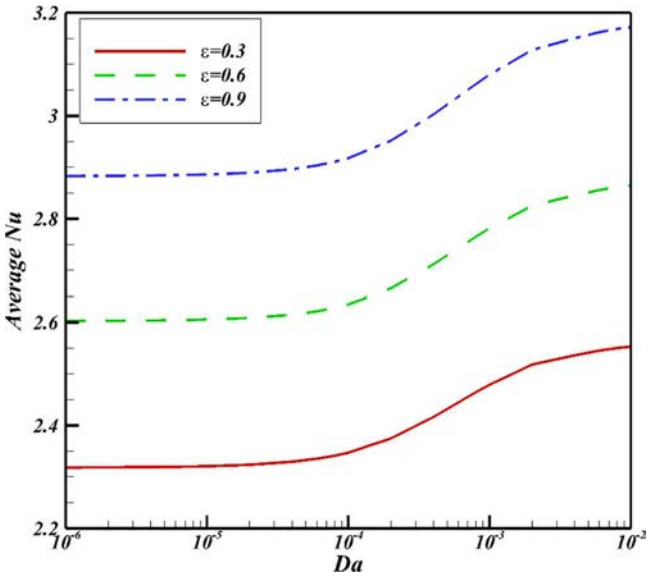

Figure 5. The effect of varying porosity on average Nusselt number for different *Da; Ra* = 10^3, *Pr* = *10, Le* = 10^3, η = 0.8, Nhs = 5, Ψ = 90°, $\zeta_1 = \zeta_2 = 0.5$, $N_b = 2.5 \times 10^{-4}$, $N_t = 10^{-4}$, $N_r = 5$, $L_p = S_p = 0.5$.

impact of such variation on average Nusselt number $\overline{Nu}$, which is extremely important in heat and mass transfer phenomena, has been investigated.

The variation of average Nusselt number of the left vertical wall with the angle of porous fin for different Brownian and thermophoresis parameters (N_b and N_t) is depicted in Figure 4. As seen in Figure 4, the value of the average Nusselt number, in the cases for which the porous fin angle is between 50 and 90, is larger than in the others. In fact, when Ψ is lower than 90, the porous fin affects the main circulation formed in the middle of the cavity and causes an increase in Nusselt number particularly when $L_p = 0.5$. Furthermore, in the cases for which $\Psi > 90$, the value of $\overline{Nu}$ drops noticeably. Moreover, the impact of varying the parameters N_b and N_t on average Nusselt number

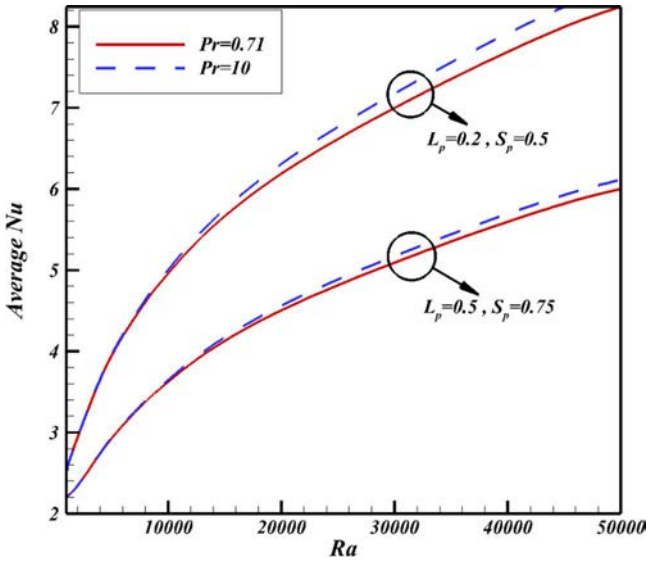

Figure 6. The effect of *Ra* and *Pr* numbers on average Nusselt number for different positions and length of the porous fin; *Da* = 10^{-3}, *Le* = 10^3, η = 0.8, Nhs = 5, Ψ = 90°, $\zeta_1 = \zeta_2 = 0.5$, $N_b = 2.5 \times 10^{-4}$, $N_t = 10^{-4}$, $N_r = 5$, ε = *0.3*.

is dependent on the angle of the porous fin. As an illustration, the value of $\overline{Nu}$ is an increasing function of N_t at $\Psi = 60$ and a decreasing function of N_t at $\Psi = 80$.

It is worth mentioning that the alteration of certain non-dimensional parameters such as *Le*, $\zeta 1$, $\zeta 2$, and *Nhs* had no significant effect on heat transfer in this study. Therefore, the effect of these parameters on heat transfer has not been shown, for brevity.

The effect of Darcy number on average Nusselt number for different porosity values is presented in Figure 5.

In accordance with Figure 5, when Darcy number is low ($Da < 4 \times 10^{-5}$), the variation of *Da* has no significant effect on average Nusselt number and it practically remains constant. Nevertheless,

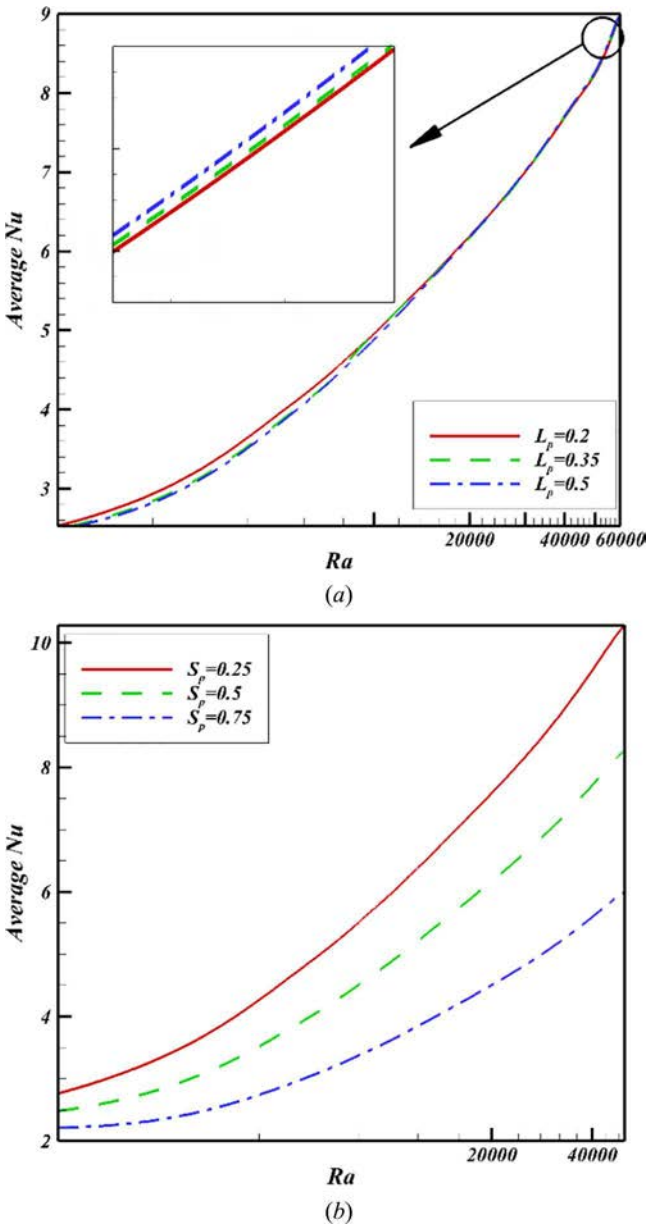

Figure 7. The influence of L_p (a) and S_p (b) on the average Nusselt number for different Rayleigh numbers; $Da = 10^{-3}$, Pr = 10, $Le = 10^3$, $\eta = 0.8$, Nhs = 5, $\Psi = 90°$, $\zeta_1 = \zeta_2 = 0.5$, $N_b = 2.5 \times 10^{-4}$, $N_t = 10^{-4}$, $N_r = 5$, $\varepsilon = 0.3$: a) $S_p = 0.5$ and b) $L_p = 0.5$.

average Nusselt number rises as the value of Darcy number becomes greater than 4×10^{-5} and the slope of this increasing function drops considerably as *Da* becomes larger than 2×10^{-3}. In addition, the higher the porosity, the higher the average Nusselt number. In essence, according to Eq. (23), porosity plays the role of the coefficient for conductivity, thermophoresis, and Brownian phenomena in this study and as a result, any augmentation of ε will increase heat transfer.

The average Nusselt number for various values of Rayleigh number, Prandtl number, L_p, and S_p is shown in Figure 6.

As shown in Figure 6, increase in *Ra* causes the average Nusselt number to increase drastically. In fact, any increase in Rayleigh number is responsible for the dominance of convective heat transfer with respect to conduction and consequently, for increase in $\overline{Nu}$. Moreover, it is shown that the average Nusselt number is an augmenting function of Prandtl number. In fact, for high values of *Pr*, the viscous diffusion rate becomes greater than the thermal diffusion rate and consequently convection is very effective in transferring energy in comparison to pure conduction; hence the average Nusselt number is high in such cases. Further, variation of the length and position of the porous fin influences the value of $\overline{Nu}$. Therefore, for further investigation, the value of average Nusselt number for different S_p and L_p parameters is demonstrated in Figure 7.

As shown in Figure 7, the impact of varying the position of the porous fin on average Nusselt number is noticeably greater than that of fin length. It is shown that in contrast to low values of *Ra*, for high values of Rayleigh number, as the parameter L_p rises Nusselt number increases. Moreover, average Nusselt number is a decreasing function of fin position. It can be deduced that when the flow circulation in the cavity is clockwise and reaches the left vertical boundary, the presence of the porous fin causes enhancement in heat transfer; and therefore, the lower the fin position, the more the temperature gradient in the left vertical wall increases and markedly affects average Nusselt number. In other words, when the porous fin is attached to the top of the left vertical wall ($S_p = 0.75$), the non-dimensional temperature gradient through the left boundary does not increase to where nanofluid flow reaches the fin and consequently, the average temperature gradient ($\overline{Nu}$) becomes lower than in the other two cases.

Finally, the effect of variation of the thermal conductivity ratio (η) on the average Nusselt number $\overline{Nu}$ for different Rayleigh numbers is shown in Figure 8.

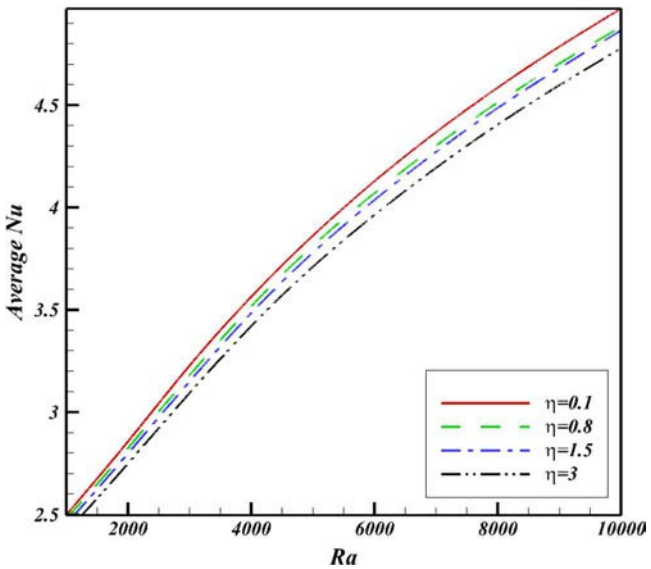

Figure 8. The impact of thermal conductivity ratio (η) on average Nusselt number for different Rayleigh numbers; $Pr = 10$, $L_p = S_p = 0.5$, $Da = 10^{-3}$, $Le = 10^3$, Nhs = 5, $\Psi = 90°$, $\zeta_1 = \zeta_2 = 0.5$, $N_b = 2.5 \times 10^{-4}$, $N_t = 10^{-4}$, $N_r = 5$, $\varepsilon = 0.3$.

Following the variations in Figure 8, it is shown that the average Nusselt number is a decreasing function of the thermal conductivity ratio. Moreover, it seems that the influence of the variation of the parameter η on the average Nusselt number $\overline{Nu}$ is more noticeable for high values of the Rayleigh number compared with lower ones.

7. Conclusion

Considering a local non-equilibrium thin porous fin attached to an enclosure wall, a laminar natural convection of nanofluid is investigated. It is assumed that the cavity walls are non-conducting and impermeable to the nanoparticles and the porous medium is isotropic and homogenous. Moreover, the vertical walls are assumed to be isothermal and the horizontal ones are assumed adiabatic. The effects of varying many crucial parameters such as Rayleigh number, Darcy number, Prandtl number, porosity, fin position, fin angle, and fin length on the heat transfer are studied. It is shown that the average Nusselt number of the left vertical wall is an increasing function of Rayleigh number and for low values of Darcy number it remains constant and then gradually increases by augmentation of *Da*. Furthermore, the greater the increase in porosity and Prandtl number, the higher the average Nusselt number $\overline{Nu}$. In addition, the value of average Nusselt number strongly depends on the fin angle in which firstly, for low angles it is high, then suddenly drops by increasing Ψ. Eventually, it is shown that, in contrast to the fin position in which the heat transfer ascends by the reduction of S_p, the behavior of $\overline{Nu}$ due to variation in fin length depends on Rayleigh number. Eventually, any increase in the thermal conductivity ratio parameter η leads to a decrease in the value of $\overline{Nu}$.

Acknowledgments

The first and second authors acknowledge the financial support of Dezful Branch, Islamic Azad University, Dezful, Iran. The first, second, and third authors are grateful to Iran Nanotechnology Initiative Council (INIC) for financial support of the present study. The authors gratefully acknowledge the Sheikh Bahaei National High Performance Computing Center (SBNHPCC) for providing computing facilities and time. SBNHPCC is supported by the Scientific and Technological Department of the Presidential Office and Isfahan University of Technology (IUT).

References

[1] D. V. Davis, Natural Convection of Air in a Square Cavity: A Benchmark Numerical Solution, *Int. J. Numer. Methods Fluids*, vol. 3, pp. 249–264, 1983.
[2] P. LeQuéré, Accurate Solution to the Square Thermally Driven Cavity at High Rayleigh Number, Comput. Fluids, vol. 20, pp. 29–41, 1991.
[3] S. Ostrach, Natural Convection in Enclosures, Adv. Heat Transf., vol. 8, pp. 161–227, 1972.
[4] R. L. Frederick and A. Valencia, Heat Transfer in a Square Cavity with a Conducting Partition on its hot wall, Int. Commun. Heat Mass Transf., vol. 16, pp. 347–354, 1989.
[5] R. Scozia and R. L. Frederick, Natural Convection in Slender Cavities with Multiple fins Attached on an Active Wall, Numer. Heat Transf. Part A, vol. 20, pp. 127–158, 1991.
[6] G. N. Facas, Natural Convection in a Cavity with fins Attached to both Vertical Walls, J. Thermophys. Heat Transf., vol. 7, pp. 555–560, 1993.
[7] A. Nag, A. Sarkar, and V. M.K. Sastri, Natural Convection in a Differentially Heated Square Cavity with a Horizontal Partition Plate on the hot Wall, Comput. Methods Appl. Mech. Eng., vol. 110, pp. 143–156, 1993.
[8] E. K. Lakhal, M. Hasnaoui, E. Bilgen, and P. Vasseur, Natural Convection in Inclined Rectangular Enclosures with Perfectly Conducting Fins Attached on the Heated Wall, Heat Mass Transf., vol. 32, pp. 365–373, 1997.
[9] K. Khanafer, A. AlAmiri, and J. Bull, Laminar Natural Convection Heat Transfer in a Differentially Heated Cavity with a thin Porous fin Attached to the Hot Wall, Int. J. Heat Mass Transf., vol. 87, pp. 59–70, 2015.
[10] X. Shi and J. M. Khodadadi, Laminar Natural Convection Heat Transfer in a Differentially Heated Square Cavity due to a thin fin on the Hot Wall, ASME J. Heat Transf., vol. 125, pp. 623–634, 2003.
[11] P. Oosthuizen, and J. T. Paul Free Convection Heat Transfer in a Cavity Fitted with a Horizontal Plate on the Cold Wall, in: S. M. Shenkman, et al. (eds.), Advances in Enhanced Heat Transfer, ASME-HTD, vol. 43, pp. 101–107, 1985.

[12] E. Bilgen, Natural Convection in Cavities with a thin fin on the Hot Wall, Int. J. Heat Mass Transf., vol. 48, pp. 3493–3505, 2005.
[13] A. Ben-Nakhi and A. Chamkha, Conjugate Natural Convection in a Square Enclosure with inclined thin fin of Arbitrary Length, Int. J. Therm. Sci. Int. J. Therm. Sci., vol. 46, pp. 467–478, 2007.
[14] A. Ben-Nakhi and A. J. Chamkha, Effect of Length and Inclination of a Thin Fin on Natural Convection in a Square Enclosure, Numer. Heat Transf., Part A, vol. 50, pp. 381–399, 2006.
[15] A. Ben-Nakhi and A. J. Chamkha, Conjugate Natural Convection Around a Finned Pipe in a Square Enclosure with Internal Heat Generation, Int. J. Heat Mass Transf., vol. 50, pp. 2260–2271, 2007.
[16] N. Ben Cheikh, A. J. Chamkha, and B. Ben Beya, Effect of Inclination on Heat Transfer and Fluid Flow in a Finned Enclosure Filled with a Dielectric Liquid, Numer. Heat Transf. Part A, vol. 56, pp. 286–300, 2009.
[17] A. J. Chamkha, M. A. Mansour, and S. E. Ahmad, Double-Diffusive Natural Convection in Inclined Finned Triangular Porous Enclosures in the Presence of Heat Generation/Absorption Effects, Heat Mass Transf., vol. 46, pp. 757–768, 2010.
[18] Y. Varol, H. F. Oztop, F. O. Ozgen, and A. Koca, Experimental and Numerical Study on Laminar Natural Convection in a Cavity Heated from Bottom due to an inclined fin, Heat Mass Transf., vol. 48, pp. 61–70, 2012.
[19] A. C. Baytas and I. Pop, Free Convection in a Square Porous Cavity using a Thermal Nonequilibrium Model, Int. J. Thermal Sci., vol. 41, pp. 861–870, 2002.
[20] D. B. Ingham and I. Pop (Eds), Transport Phenomena in Porous Media III, Elsevier, Oxford, 2005.
[21] K. Vafai Handbook of Porous Media, 2nd edn. Taylor and Francis, New York, 2005.
[22] L. Zhang, Y. Ding, M. Povey, and D. York, ZnO Nanofluids–a Potential Antibacterial Agent, Progress in Natural Sci., vol. 18, pp. 939–944, 2008.
[23] K. Hirota, M. Sugimoto, M. Kato, K. Tsukagoshi, T. Tanigawa, and H. Sugimoto, Preparation of Zinc Oxide Ceramics with a Sustainable Antibacterial Activity under Dark Conditions, Ceramics Int., vol. 36, pp. 497–506, 2010.
[24] C. Choi, H. S. Yoo, and J. M. Oh, Preparation and Heat Transfer Properties of Nanoparticle-Intransformer oil Dispersions as Advanced Energy-Efficient Coolants, Current Appl Physics, vol. 8, pp. 710–712, 2008.
[25] J. L. Davidson Nanofluid for Cooling Enhancement of Electrical Power Equipment, Vanderbilt University-Department of Electrical Engineering, Nashville, TN, www.vanderbilt.edu/technology transfer Bulletin, 2009.
[26] K. Khanafer and K. Vafai, A Critical Synthesis of Thermophysical Characteristics of Nanofluids, Int. J. Heat Mass Transf., vol. 54, pp. 4410–4428, 2011.
[27] J. Buongiorno, Convective Transport in Nanofluids, J. Heat Transf., vol. 128, pp. 240, 2006.
[28] D. A. Nield and A. V. Kuznetsov, Thermal Instability in a Porous Medium Layer Saturated by a Nanofluid, Int. J. Heat Mass Transf., vol. 52, pp. 5796–5801, 2009.
[29] H. Zargartalebi, A. Noghrehabadi, and M. Ghalambaz, Ioan Pop, Natural Convection Boundary Layer Flow over a Horizontal Plate Embedded in Porous Medium Saturated with a Nanofluid: Case of Variable Thermophysical Properties, Transp. in Porous Media, vol. 107, pp. 153–170, 2014.
[30] D. Y. Tzou, Instability of Nanofluids in Natural Convection, J. Heat Transf., vol. 130, pp. 072401, 2008.
[31] D. Y. Tzou, Thermal Instability of Nanofluids in Natural Convection, Int. J. Heat Mass Transf., vol. 51, pp. 2967–2979, 2008.
[32] D. A. Nield and A. V. Kuznetsov, The Cheng–Minkowycz Problem for Natural Convective Boundary-Layer Flow in a Porous Medium Saturated by a Nanofluid, Int. J. Heat Mass Transf., vol. 52, pp. 5792–5795, 2009.
[33] H. Zargartalebi, M. Ghalambaz, A. Noghrehabadi, and A. Chamkha, Stagnation-Point Heat Transfer of Nanofluids towards Stretching Sheets with Variable Thermo-Physical Properties, Advanced Powder Tech., vol. 26, pp. 819–829, 2015.
[34] B. Alazmi and K. Vafai, Analysis of Fluid Flow and Heat Transfer Interfacial Conditions between a Porous Medium and a Fluid Layer, Int. J. Heat Mass Transf., vol. 44, pp. 1735–1749, 2001.
[35] K. Yang and K. Vafai, Restrictions on the Validity of the Thermal Conditions at the Porous-Fluid Interface: An Exact Solution, ASME J. Heat Transf., vol. 133, pp. 112601, 2011.
[36] J. N. Reddy, *An Introduction to the Finite Element Method*, McGraw-Hill, New York, 1993.
[37] T. Basak, S. Roy, and A. R. Balakrishnan, Effects of Thermal Boundary Conditions on Natural Convection flows within a Square Cavity, Int. J. Heat Mass Transf., vol. 49, pp. 4525–4535, 2006.
[38] T. Basak, S. Roy, T. Paul, and I. Pop, Natural Convection in a Square Cavity Filled with a Porous Medium: Effects of Various Thermal Boundary Conditions, Int. J. Heat Mass Transf., vol. 49, pp. 1430–1441, 2006.